



Received Date : 24-Sep-2018

Revised Date : 19-Nov-2018

Accepted Date : 19-Nov-2018

Article type : Research Letter

Environmental pH and Glu364 to Gln mutation in the chlorophyll-binding CP47 protein affect redox-active TyrD and charge recombination in Photosystem II

Jaz N. Morris^{1,3}, Sándor Kovács², Imre Vass², Tina C. Summerfield¹, Julian J. Eaton-Rye³

1 Department of Botany, University of Otago, Dunedin, New Zealand

2 Institute of Plant Biology, Biological Research Centre of the Hungarian Academy of Sciences, Szeged, Hungary

3 Department of Biochemistry, University of Otago, Dunedin, New Zealand

Correspondence

J.J. Eaton-Rye, Department of Biochemistry, University of Otago, P.O. Box 56, Dunedin 9054, New Zealand

Fax: +63 3 479 7865

Tel: +64 3 479 7866

Email: julian.eaton-rye@otago.ac.nz

This article has been accepted for publication and undergone full peer review but has not been through the copyediting, typesetting, pagination and proofreading process, which may lead to differences between this version and the Version of Record. Please cite this article as doi: 10.1002/1873-3468.13307

This article is protected by copyright. All rights reserved.

Accepted Article

In Photosystem II, loop E of the chlorophyll-binding CP47 protein is located near a redox-active tyrosine, Y_D, forming a symmetrical analog to loop E in CP43, which provides a ligand to the oxygen-evolving complex (OEC). A Glu364 to Gln substitution in CP47, near Y_D, does not affect growth in the cyanobacterium *Synechocystis* sp. PCC 6803; however, deletion of the extrinsic protein PsbV in this mutant leads to a strain displaying a pH-sensitive phenotype. Using thermoluminescence, chlorophyll fluorescence, and flash-induced oxygen evolution analyses, we demonstrate that Glu364 influences the stability of Y_D and the redox state of the OEC, and highlight the effects of external pH on photosynthetic electron transfer in intact cyanobacterial cells.

Keywords: CP47; cyanobacteria; oxygen-evolving complex; Photosystem II; *Synechocystis* sp. PCC 6803; TyrD; Y_D

Abbreviations

CAPS, 3-(cyclohexylamino)-1-propanesulfonic acid; CP43, 43 kDa chlorophyll-binding core antenna protein; CP47, 47 kDa chlorophyll-binding core antenna protein; D1, PsbA reaction center protein; D2, PsbD reaction center protein; DCMU, 3,4-dichloro-1,1-dimethyl urea; HEPES, 4-(2-hydroxyethyl)-1-piperazineethanesulfonic acid; His_D, His189 of D2; His_Z, His190 of D1; OEC, oxygen-evolving complex; P₆₈₀, reaction center chlorophylls of PS II; P₇₀₀, reaction center chlorophylls of PS I; PCC, Pasteur Culture Collection; PS I, Photosystem I; PS II, Photosystem II, Q_A, primary plastoquinone electron acceptor of PS II; Q_B, secondary plastoquinone electron acceptor of PS II; S₀-S₄, oxidation states of the OEC; *Synechocystis* 6803, *Synechocystis* sp. PCC 6803; TL, thermoluminescence; Y_Z, redox-active Tyr161 of the D1 protein; Y_D, redox-active Tyr160 of the D2 protein; Y_D^(ox), oxidized form of Y_D (either Y_D⁺ or the neutral radical Y_D[•]); Y4/Y3, ratio of the O₂ yield on flash 4 to the O₂ yield on flash 3

Photosystem II (PS II) is a light-driven water-plastoquinone oxidoreductase. In PS II, excitation of the four-chlorophyll P₆₈₀ reaction center initiates a series of electron transfer steps via pheophytin to the primary and secondary plastoquinone acceptors (Q_A and Q_B, respectively) forming plastoquinol (Q_BH₂): these reactions are accompanied by the sequential extraction of electrons from water to fill the hole on P₆₈₀ via a bound Mn₄CaO₅ oxygen-evolving complex (OEC) (Shen, 2015). The PS II core complex includes the chlorophyll-binding antenna proteins CP43 and CP47 which are found adjacent to the reaction center (RC) proteins D1 and D2, respectively. In cyanobacteria the PS II core is

This article is protected by copyright. All rights reserved.

Accepted Article

surrounded by 13 low-molecular-weight membrane-spanning subunits and capped by up to four hydrophilic subunits on the luminal face of the photosystem (Ferreira et al., 2004; Umena et al., 2011; Bricker et al., 2012). A similar arrangement among the peripheral subunits is found in eukaryotic organisms and the PS II core is conserved (Ago et al., 2016; Wei et al., 2016).

Two redox-active tyrosine residues, Y_z (D1 Tyr161) and Y_D (D2 Tyr160), are located in symmetrical positions around P_{680} (Vinyard et al., 2013; Shen, 2015). During photosynthetic electron transfer, Y_z forms a neutral radical by movement of the phenolic proton towards a nearby His residue, called His_z (D1 His190). Although an analogous His residue is found adjacent to Y_D (His_D or D2 His189) the formation of the neutral Y_D radical is mediated through a water molecule that is thought to connect to a proton exit pathway involving D2 Arg180 (Styring et al., 2012; Saito et al., 2013; Nakamura and Noguchi, 2015). Upon excitation of PS II, Y_z is oxidised by P_{680} and then rapidly reduced (within μ s) by the OEC through a series of S-state transitions (where S_0 - S_4 denote oxidation states of the OEC); in contrast, oxidised Y_D ($Y_D^{(ox)}$) is stable for minutes and is not involved in water oxidation directly, but is involved in charge-equilibrium with the OEC (Kok et al., 1970; Vass et al., 1990; Rutherford et al., 2004; Styring et al., 2012; Shen, 2015). Although S_0 is the most reduced OEC state, S_1 is the dark-stable state, due to the reduction of $Y_D^{(ox)}$ to yield S_1Y_D OEC centers (Vass and Styring, 1991; Styring et al., 2012).

Both CP43 and CP47 possess six membrane-spanning helices joined by hydrophilic loops (loops A to E). In both proteins loop E is a large luminal loop, comprising \sim 130 amino acids in CP43 and \sim 190 residues in CP47 (Eaton-Rye and Putnam-Evans, 2005). While Glu354 and Arg357 of Loop E from CP43 are in the first and second coordination spheres of the OEC, respectively, a conserved Phe362-Phe363-Glu364 region in loop E of CP47 contributes to a hydrophobic pocket around Y_D (Ferreira et al., 2004). This hydrophobic pocket (Fig. 1) is thought to be important for formation of the hydrogen bond network surrounding Y_D that permits electron transfer from Y_D to P_{680}^+ ; accordingly, the hydrophobic pocket may also reduce damaging charge recombination from the PS II acceptor side (via the P_{680} RC) to the Y_D^\bullet radical, because of the lack of an available proton (Styring et al., 2012; Saito et al., 2013). Glu364 is within H-bonding distance (\sim 2.8 Å) to D2 Arg294, which coordinates His_D (Styring et al., 2012; Suga et al., 2015), and this residue might therefore be important for the release of the phenolic proton of Y_D to the available water (Saito et al., 2013; Nakamura and Noguchi, 2015; Sjöholm et al., 2017). However, in the cyanobacterium *Synechocystis* sp. PCC 6803 (hereafter *Synechocystis* 6803), CP47 Glu364 to Gln or Glu364 to Gly substitutions produced strains similar to the wild type, in contrast to severely impaired growth in a Phe363 to Arg mutant (Putnam-Evans et al., 1996; Morgan et al., 1998; Clarke and Eaton-Rye, 1998; Clarke and

Eaton-Rye, 1999). Loop E of CP47 extends into the thylakoid lumen and is involved in binding of the cyanobacterial PS II extrinsic subunit PsbO, which, along with the PsbU, PsbV and possibly CyanoQ proteins, protects the OEC and Y_D from the reductive environment of the lumen and is necessary for maximal rates of oxygen evolution (Bricker et al., 2012; Roose et al., 2016). Deletion of PsbV in the CP47 E364Q mutant of *Synechocystis* 6803 resulted in a strain displaying a pH-sensitive phenotype, in which PS II function and assembly were reduced and photoautotrophic growth was not possible at pH 7.5; however, pH 10.0 rescued growth and PS II function (Eaton-Rye et al., 2003; Summerfield et al., 2005).

A number of pH-sensitive PS II mutants of *Synechocystis* 6803 carrying deletions in PS II extrinsic proteins have been reported (Eaton-Rye et al., 2003; Summerfield et al., 2005a, 2005b, 2007, 2013), despite the physical separation of the thylakoid lumen from changes in environmental pH. To investigate possible mechanisms for this phenomenon (Morris et al., 2016), and with recent studies highlighting Glu364 as an important residue in the Y_D pocket (Saito et al., 2013; Bricker et al., 2015; Sjöholm et al., 2017), we were prompted to look again at the E364Q mutant in the context of possible redox perturbations around Y_D . In the case of the pH 7.5-non-photoautotrophic E364Q: Δ PsbV strain, we hypothesized that an altered environment around Y_D at pH 7.5 compounds the contribution of PsbV removal to pH-sensitivity. Thus, we investigated PS II activity in the E364Q and E364Q: Δ PsbV mutants, compared to wild type and the Δ PsbV strain. By determination of thermoluminescence (TL), chlorophyll *a* (hereafter chlorophyll) fluorescence decay measurements and flash-induced oxygen production, we demonstrate that CP47 Glu364 is important for charge recombination in PS II, and suggest a mechanism by which altered Y_D oxidation contributes to the pH-sensitivity of the E364Q: Δ PsbV mutant.

Materials and methods

Strains and culture conditions

Glucose-tolerant *Synechocystis* 6803 strains used in this work are listed in Table 1, and were grown using BG-11 liquid and solid media (Rippka et al., 1979) in the presence of 5 mM glucose (unless indicated otherwise) and appropriate antibiotics, and maintained at 30 °C under continuous $\sim 40 \mu\text{E m}^{-2} \text{ s}^{-1}$ illumination as described previously (Eaton-Rye, 2011). For physiological measurements, liquid cultures in mid-late logarithmic growth phase were harvested by centrifugation at $\sim 2500 \times g$, washed twice with BG-11, and resuspended in BG-11 media buffered with either 25 mM HEPES-NaOH pH 7.5 or 25 mM CAPS-NaOH pH 10.0. Cells were incubated at 5 μg chlorophyll mL^{-1} until the

initiation of measurements, after 8 or 24 h, as appropriate to the experiment. For some measurements of flash-induced oxygen evolution, 5 mM glucose was added during the incubation period.

Physiological measurements

Measurement of TL was carried out using a custom-built machine (Vass et al., 1981; Ducruet and Vass, 2009). For determination of TL, cells were subjected to 30 s of $250 \mu\text{E m}^{-2} \text{s}^{-1}$ illumination at 20 °C and 3 min dark adaptation at 20 °C prior to cooling to -20 °C, whereupon a single-turnover actinic flash was provided by a xenon flash bulb. Samples were cooled to -40 °C, and subsequently warmed to 80 °C at a rate of 20 °C min^{-1} , during which time the TL photon yield was measured. Measurements were made in the presence and absence of 20 μM 3,4-dichloro-1,1-dimethyl urea (DCMU), which was applied during the dark adaptation period. Data were analysed by curve-fitting to determine peak amplitude and peak temperatures using custom-made software, as in Cser and Vass (2007).

Flash-induced oxygen evolution was determined using a custom-built Joliot-type electrode (Joliot and Joliot, 1968) as described previously (Jackson and Eaton-Rye, 2015). Briefly, intact cells (equivalent to 2.5 μg chlorophyll) were dark adapted for 5 min in direct contact with a bare platinum cathode and illuminated with saturating single-turnover actinic flashes provided by a 617 nm LED array. Twenty flashes at 4 Hz were used, with a flash width of 4-8 μs .

Room-temperature chlorophyll fluorescence decay and induction measurements using cells dark adapted for 5 min prior to measurements were made using an FL-3000 double-modulation fluorimeter (Photon Systems Instruments, Czech Republic) using parameters previously described (Deák et al., 2014). Fluorescence decay measurements were made in the presence and absence of 20 μM DCMU added in the dark adaptation period, and fluorescence decay data were analyzed using the software Origin 2017 (OriginLab, MA, USA), using a fitting algorithm previously described (Vass et al., 1999; Cser and Vass, 2007).

The PS I oxidation state in cells was determined by P_{700} -dependent absorbance changes in the near-infrared ($A_{875 \text{ nm}} - A_{830 \text{ nm}}$) induced by illumination with 635 nm actinic light ($\sim 1000 \mu\text{E m}^{-2} \text{s}^{-1}$) (Klughammer and Schreiber, 1994) using a Dual-PAM-100 measuring system (Walz, Germany). Cells were dark adapted for 5 min prior to measurements, and data were baseline corrected and normalized to the P_{700}^+ oxidation state maxima.

Results

pH, and the Glu364 to Gln substitution, affects thermoluminescence yield and C-band stability

To assess the effects of the Glu364 to Gln mutation and pH on charge recombination in PS II, *Synechocystis* 6803 strains were incubated under photoautotrophic conditions at pH 7.5 and pH 10.0 for 8 h, and the TL from these strains was determined. In dark-adapted PS II following a single-turnover actinic flash, charge recombination produces characteristic TL bands from $S_2Q_B^-$ (B band), $S_2Q_A^-$ (Q band – occurs in the presence of DCMU), and $Y_D^{(ox)}Q_A^-$ (C band – may occur whether DCMU is present or not) charge pairs (Arnold and Sherwood, 1957; Sane, 2004; Cser and Vass, 2007; Ducruet and Vass, 2009). The wild type and the Δ PsbV, E364Q and E364Q: Δ PsbV strains typically displayed enhanced TL yield from B and Q bands at pH 7.5 compared to pH 10.0, and increased C band yield (in the presence and absence of DCMU) at pH 10.0 compared to pH 7.5, indicating increased charge recombination between the quinone acceptors and the OEC at low pH and increased recombination between $Y_D^{(ox)}$ and Q_A^- at higher pH (Figure 2, Table 2). However, the B band TL yield was similar at both pH values for wild type and the B band yield was larger at pH 10 than pH 7.5 in E364Q cells (Fig. 2A; Table 2). In addition, in the presence of DCMU, the intensity of the C band in the Δ PsbV strain was somewhat larger at pH 7.5 than at pH 10 while the C band was similar at both pH values in E364Q: Δ PsbV cells (Fig. 2D, Table 2). Strikingly, the E364Q mutant emitted B, Q and C band TL at a much greater level than wild-type cells, and both mutants lacking PsbV had reduced TL yield, likely due to reduced PS II levels in these strains (Eaton-Rye et al., 2003). Moreover, C-band yield was enhanced in E364Q: Δ PsbV cells in the presence of DCMU compared to Δ PsbV cells, indicating an increased population of $Y_D^{(ox)}Q_A^-$ in these mutants. Furthermore, the temperatures of TL peak maxima (T_{max} , which indicates the activation energy required to cause charge recombination and hence charge pair stability) were similar for B and Q bands in wild type, and for the B band in the Δ PsbV strain, between pH levels, but both mutants carrying the Glu364 to Gln substitution showed enhanced B and Q band stability at pH 10.0. Compared to the wild type, all mutants showed enhanced Q band T_{max} ($S_2Q_A^-$ stability), with an apparent additive effect from the Glu364 to Gln substitution and removal of PsbV in the E364Q: Δ PsbV double mutant. Similar to TL yield, the C band T_{max} was generally enhanced at pH 10.0 in the presence and absence of DCMU, indicating an increase in $Y_D^{(ox)}Q_A^-$ stability at higher pH.

The Glu364 to Gln substitution impairs back reactions of PS II independently of the PsbV deletion

Chlorophyll fluorescence decay following a single-turnover actinic flash can be used to probe reoxidation of Q_A^- in PS II by Q_B or by the OEC (Robinson and Crofts, 1983; Cser and Vass, 2007), and was measured in tandem with TL (Fig. 3, Table 3). In wild-type cells the chlorophyll decay kinetics consist of a fast phase (μ s) reflecting the oxidation of Q_A^- by bound Q_B , a medium phase (ms) that is thought to arise from Q_A^- oxidation in centers where Q_B was not bound before the actinic flash and a slow phase (s) which corresponds to the back reaction with the S_2 state of the OEC (Vass et al., 1999). At pH 7.5 the fast phase of the fluorescence decay was slightly slowed in the E364Q cells when compared to wild type but the medium phase was similar, suggesting the Q_B binding site properties were also similar in wild type and the E364Q mutant. In contrast, the slow phase in the E364Q strain exhibited a $t_{1/2}$ of 9.5 s compared to 1.3 s in the wild type although both had similar amplitudes (Table 3). A similar trend was seen between these two strains when the chlorophyll decay was measured in cells grown and measured at pH 10.0 but in this instance the amplitude of the slow phase increased from 15% to 18% in the E364Q cells while it decreased in wild type to 11%.

The chlorophyll fluorescence decay kinetics in the Δ PsbV strain also exhibited slowed fast and slow components relative to wild type; however, the Δ PsbV strain also had a slowed middle phase (e.g., from 1.5 ms in wild type to 5.1 ms in Δ PsbV cells at pH 7.5 and a similar change was evident at pH 10.0 (Table 3)). Strikingly the E364Q: Δ PsbV double mutant exhibited kinetics more closely resembling the wild type than either single mutant although the slow component at pH 7.5 had an elevated amplitude (24% in E364Q: Δ PsbV cells; 15% in wild type) and there was a corresponding decrease in the amplitude of the fast component in the E364Q: Δ PsbV strain (Table 3).

In the presence of DCMU the decay of chlorophyll fluorescence can be fit by a millisecond component and a slow seconds components (Vass et al., 1999). In Table 3 the slow component is extended by approximately a factor of 2 relative to wild type in all mutants and a slowed decay is observed in Fig. 3C,D. A large pH effect on the fast phase, however, was evident in E364Q cells (4.1 ms (3%) at pH 7.5 and 0.5 ms (2%) at pH 10.0). The millisecond component in wild type by comparison was 2.5 (2%) at pH 7.5 and 1.3 ms (3%) at pH 10.0, while in the Δ PsbV strain it remained constant at approximately 5 ms but with slightly increased amplitude at pH 10.0 (Table 3). Interestingly, in the case of the E364Q: Δ PsbV double mutant, the millisecond component more closely resembled the rate observed at pH 10.0 for the E364Q strain (Table 3). In addition, when PsbV was absent the chlorophyll decays did not reach zero and this effect was most pronounced in the E364Q: Δ PsbV mutant in the presence of DCMU at pH 7.5 (Fig. 3B,D). This suggests a reduced dark S_1 stable fraction of the OEC in Δ PsbV and E364Q: Δ PsbV cells.

The dark S state population of PS II is altered by the removal of PsbV and the Glu364 to Gln substitution

In order to assess the redox state of the PS II OEC following dark adaptation, measurements of flash-induced oxygen evolution were made using a Joliot-type electrode. In one experiment, wild type and mutant cells were incubated for 24 h in pH 7.5 mixotrophic conditions permissive for growth in all strains (Fig. 4A). Charge recombination during 5 min dark adaptation leads to a population of PS II with mixed OEC S states of around 25% $S_0Y_D^{(ox)}$ /75% S_1Y_D (Vass and Styring, 1991); thus, a distinct peak in oxygen evolution occurs following three single-turnover flashes (from OEC centers in an initial dark S_1 state), and a somewhat reduced 4th flash yield (initial S_0 state). In wild type, a typical flash-induced oxygen evolution pattern was observed. However, a shift in the relative oxygen evolution favoring 4th flash oxygen evolution in cells lacking PsbV was observed with an increase in the S_0 population observed in both Δ PsbV and E364Q: Δ PsbV cells relative to wild type and the E364Q strain, respectively (Table 4). Impaired photoautotrophic growth and oxygen evolution in strains lacking the PsbV protein meant that flash oxygen yield comparisons in pH 7.5/10.0 photoautotrophic conditions were made only in the wild type and E364Q strains in a subsequent experiment (Fig. 4B). As in the case of mixotrophic growth, flash oxygen yields were somewhat reduced in the E364Q mutant compared to wild type, in particular at pH 10.0. Whereas the normalized 4th flash/3rd flash yield from the wild type was similar between pH levels, the yield from the E364Q strain compared to wild type was apparently more variable, reduced at pH 7.5, and elevated at pH 10.0 (Table 4). In comparison to wild type the S_0 state was also increased in E364Q cells at both pH values (Table 4) revealing an increased population of a dark S_0 state in the E364Q mutant, rather than S_1 .

The analysis of the oxygen evolution parameters in Table 4 additionally found the level of misses and double hits to be similar between the strains under mixotrophic conditions; however, under photoautotrophic conditions, E364Q cells exhibited a reduction in misses at pH 7.5 and an increase in double hits at pH 10.0. Furthermore, the number of active PS II centers in the dark-adapted cells, in any of the strains, was reduced relative to wild type in the mixotrophically grown cells and the number of active centers at pH 10.0 relative to pH 7.5 in both wild type and the E364Q strain declined. It should be noted that steady-state oxygen evolution and PS II assembly have been shown to be similar in wild type and E364Q cells at pH 7.5 and pH 10.0 but the removal of PsbV (in cells grown at pH 7.5 or in unbuffered BG-11) in either background reduced the number of PS II centers by approximately 55% and 65%, respectively (Morgan et al., 1998; Eaton-Rye et al., 2003; Summerfield et al., 2005).

The Glu364 to Gln substitution does not substantially alter room temperature PS II fluorescence induction or low-temperature fluorescence; pH alters the rate of reduction of PS I

Variable chlorophyll fluorescence arising from PS II was induced in dark-adapted cells by actinic light; wild type and E364Q cells showed a typical fluorescence induction 'OJIP' curve (Papageorgiou and Govindjee, 2011; Kaňa et al., 2012). Greater variable fluorescence was observed in all strains at pH 10.0 relative to pH 7.5 following 8 h incubation, particularly in the E364Q mutant (Fig. 4C). Deletion of *PsbV* reduced fluorescence yield; this effect was enhanced by the Glu364 to Gln mutation in the E364Q:Δ*PsbV* double mutant. Measurements of low-temperature (77 K) fluorescence reflected similar differences between strains (Supporting Information Fig. S3), wherein fluorescence at pH 7.5 with 440 nm (targeting chlorophyll) and 580 nm (targeting phycobilisomes) excitation wavelengths reflected a reduction in assembled PS II and decreased accessory pigment coupling, respectively, in Δ*PsbV* and E364Q:Δ*PsbV* cells.

The net effect of PS II function in terms of electron transport to PS I can be inferred from analysis of P_{700} oxidation kinetics (Fig. 4D). Actinic illumination of dark-adapted cells results in a prompt change in absorbance in the near infrared due to oxidation of P_{700} , which appears as a signal increase. Quenching of the signal then occurs due to reduction of PS I by electron transport from PS II and/or cyclic electron transport via the cytochrome *b₆f* complex (Klughammer and Schreiber, 1994). At pH 10.0, enhanced electron transport to PS I was observed in all strains relative to pH 7.5, with greater and generally more rapid quenching of P_{700}^+ after ~0.5 s. In E364Q cells, P_{700}^+ was apparently quenched more rapidly than in the wild type, but deletion of *PsbV* both slowed and reduced the ability of electron transport to reduce P_{700}^+ . This effect was greater in the E364Q:Δ*PsbV* double mutant, and it is noted that the limited variable chlorophyll fluorescence and P_{700}^+ quenching observed in these experiments both indicate functional electron transport in this mutant, but this is presumably insufficient to maintain pH 7.5 photoautotrophic growth.

Discussion

The Glu364 to Gln substitution affects PS II electron transfer processes, due to an effect on Y_D

Previous studies of loop E in CP47 identified amino acid residues that are now known to be located adjacent to Y_D (Ferreira et al., 2004; Umena et al., 2011; Suga et al., 2015) that were important for PS II assembly and function (Eaton-Rye and Vermaas, 1991; Clarke and Eaton-Rye, 1999). Among these a Glu364 to Gln substitution in CP47 appeared to produce only a minor phenotype, but the inability

of an E364Q:ΔPsbV double mutant to grow photoautotrophically indicated the importance of this residue (Putnam-Evans et al., 1996; Morgan et al., 1998). Although the Glu364 to Gln substitution did not substantially affect growth and oxygen evolution in the earlier studies, this study has unmasked potentially deleterious changes in PS II electron transfer processes in the E364Q strain, which we attribute to alterations in the H-bonding network around Y_D (Fig. 1). The striking increase in TL yield in the E364Q mutant (Fig. 2A,C; Table 2) suggests an increased probability that P_{680}^* is repopulated during charge recombination in this strain with the likely consequence that the efficiency of non-radiative charge recombination would be reduced (Cser and Vass, 2007). This might arise as a result of a destabilization of the interaction of D2 Arg294 with D2 His189 in the E364Q mutant modifying the formation of the neutral radical (Y_D^*). Such a situation would reduce the capacity of Y_D to reduce P_{680}^+ and could increase C band emission, as well as B and Q band emissions, in the E364Q strain. Certainly, an increased overall TL emission from E364Q cells compared to wild type points to modified redox potentials for specific S states or for the quinone electron acceptors resulting in altered stabilisation of the $S_2Q_B^-/S_2Q_A^-$ states. However, a shift in TL peak temperatures in E364Q cells in both the presence and absence of DCMU points to a change on the donor side of PS II rather than an alteration in the vicinity of Q_A or Q_B (Vass and Govindjee, 1996).

A perturbed H-bonding network destabilises Y_D and alters the dark equilibration of the S-states

The increased amplitude of the C band indicates the enhanced formation of $Y_D^{(ox)}Q_A^-$ by the Glu364 to Gln substitution. In addition, in the oxygen yield measurements (Fig. 4A,B), an apparent shift towards the S_0 state following a brief (~5 min) dark adaption in the photoautotrophically grown E364Q cells and in the E364Q:ΔPsbV strain was evident, particularly in the double mutant, and this could also arise from altered conformation of the Y_D pocket by perturbation of the H-bond network that ordinarily links Glu364 to His_D (via D2 Arg294), affecting the proton-transfer-coupled formation of Y_D^* (Styring et al., 2012; Saito et al., 2013; Nakamura and Noguchi, 2015; Sjöholm et al., 2017). This would lead to an increased fraction of centers in S_0 after dark adaptation by reduction in the relative proportion of S_1Y_D in favor of $S_0Y_D^{(ox)}$. Or, formation of an unstable S_1Y_D would yield OEC centers that become S_2Y_D following a flash but that recombine to $S_1Y_D^{(ox)}$ rapidly, perhaps within the time scale of the Joliot electrode flash frequency (Vass et al., 1990). The enhancement of TL emission arising from $Y_D^{(ox)}Q_A^-$ in the Glu364 to Gln mutants is consistent with this hypothesis; rapid decay of S_2 to S_1 following a flash would yield an increase in $Y_D^{(ox)}$ as the donor side recombination partner for acceptor side Q_A^- , which cannot recombine with S_1 . Deletion of PsbV in *Thermosynechococcus elongatus* also resulted in an increase in the fraction of centers in the dark S_0 state in another study,

prompting the suggestion that PsbV binding might also affect Y_D oxidation (Kirilovsky et al., 2004); this would imply a twofold effect on Y_D in the E364Q: Δ PsbV mutant.

External pH affects electron-transfer processes within PS II in intact cells

The external pH affected TL, variable chlorophyll fluorescence induction and the chlorophyll fluorescence decay kinetics following a single actinic flash in all *Synechocystis* 6803 strains, including the wild type. Likewise, the combined effect of linear and cyclic electron transfer on $P700^+$ re-reduction was enhanced at pH 10.0 relative to pH 7.5 (Fig. 4D). This is in spite of the prevailing theory that the thylakoid lumen is approximately 2 pH units lower than the cytosolic pH (Belkin et al., 1987; Belkin and Packer, 1988), which is well buffered, varying between pH \sim 6.8-7.2 in *Synechocystis* 6803 at an external pH of 8.0-10.0, respectively (Jiang et al., 2013). In isolated thylakoids, TL analysis indicates that $Y_D^{(ox)}Q_A^-$ stability increases from pH \sim 7.5 to \sim 10.0 (Vass and Inoue, 1986), and our results indicate $Y_D^{(ox)}Q_A^-$ stability was also potentially stabilized in wild type, as judged by the increased amplitude for the C band in the presence of DCMU and an increase in T_{max} in the absence of DCMU (Table 2). The impact of pH on $Y_D^{(ox)}Q_A^-$ stability was most evident in E364Q cells whereupon increasing the pH from 7.5 to 10.0 increased both the T_{max} and amplitude of the C band both in the presence and absence of DCMU (Table 2). Additionally, an increase in both the B and Q band T_{max} values for E364Q and E364Q: Δ PsbV cells at pH 10.0 also indicates that the external pH can influence the stability of both $S_2Q_A^-$ and $S_2Q_B^-$. It is possible that despite the buffering capacity of the cytosol the thylakoid lumen does become more alkaline when cells are in pH 10.0 media. This could help maintain the S_1/S_0 ratio in the dark to favor a more stable OEC (Vass and Styring, 1991; Styring et al., 2012). This might counteract the effects of the Glu364 to Gln mutation and/or the loss of PsbV leading to the enhanced rates of electron transport observed in Fig. 4D and the reactivation of photoautotrophic growth in E364Q: Δ PsbV cells at pH 10.0 (Eaton-Rye et al., 2003).

Acknowledgements

We thank Dr Simon A. Jackson for assistance with use of the Joliot electrode, and László Sass for assistance with the operation of thermoluminescence-measuring equipment and the analysis of the O_2 flash patterns. JNM was supported by the Senior Smeaton Prize in Experimental Science at the University of Otago. The laboratory of IV is supported by grant number NKFI-H (NN-110960) and GINOP-2.3.2-15-2016-00001.

This article is protected by copyright. All rights reserved.

Author contributions

JNM, IV, TCS and JER designed the experiments, and JNM and SK conducted the experimental work. JNM analysed the data and wrote the manuscript; all authors contributed to discussions about data interpretation, and had direct input on manuscript content and editing, before submission.

References

- Ago, H., Adachi, H., Umena, Y., Tashiro, T., Kawakami, K., Kamiya, N., Tian, L., Han, G., Kuang, T., Liu, Z., Wang, F., Zou, H., Enami, I., Miyano, M., and Shen, J.-R. (2016) Novel features of eukaryotic Photosystem II revealed by its crystal structure analysis from a red alga. *Journal of Biological Chemistry* 291, 5676–5687.
- Arnold, W., and Sherwood, H. K. (1957). Are chloroplasts semiconductors? *Proceedings of the National Academy of Sciences U.S.A.* 43, 105–114.
- Belkin, S., Mehlhorn, R. J., and Packer, L. (1987). Proton gradients in intact cyanobacteria. *Plant Physiology* 84, 25–30.
- Belkin, S., and Packer, L. (1988). Determination of pH gradients in intact cyanobacteria by electron spin resonance spectroscopy. *Methods in Enzymology* 167, 677–685.
- Bricker, T. M., Mummadisetti, M. P., and Frankel, L. K. (2015). Recent advances in the use of mass spectrometry to examine structure/function relationships in photosystem II. *Journal of Photochemistry and Photobiology B: Biology* 152, 227–246.
- Bricker, T. M., Roose, J. L., Fagerlund, R. D., Frankel, L. K., and Eaton-Rye, J. J. (2012). The extrinsic proteins of Photosystem II. *Biochimica et Biophysica Acta - Bioenergetics* 1817, 121–142.
- Clarke, S.M. and Eaton-Rye, J.J. (1998). Characterization of the double mutant FF362,363RR in loopE of the Photosystem II chlorophyll-binding protein CP47, in *Photosynthesis: Mechanisms and Effects*, ed. G. Garab (Kluwer Academic Publishers), Vol II. 1459–1462.
- Clarke, S. M., and Eaton-Rye, J. J. (1999). Mutation of Phe-363 in the Photosystem II protein CP47 impairs photoautotrophic growth, alters the chloride requirement, and prevents photosynthesis in the absence of either PSII-O or PSII-V in *Synechocystis* sp. PCC 6803. *Biochemistry* 38, 2707–2715.
- Cser, K., and Vass, I. (2007). Radiative and non-radiative charge recombination pathways in

This article is protected by copyright. All rights reserved.

Photosystem II studied by thermoluminescence and chlorophyll fluorescence in the cyanobacterium *Synechocystis* 6803. *Biochimica et Biophysica Acta - Bioenergetics* 1767, 233–243.

Deák, Z., Sass, L., Kiss, É., and Vass, I. (2014). Characterization of wave phenomena in the relaxation of flash-induced chlorophyll fluorescence yield in cyanobacteria. *Biochimica et Biophysica Acta - Bioenergetics* 1837, 1522–1532.

DeLano, W. L. (2001). The PyMOL molecular graphics system, DeLano Scientific, Palo Alto, CA, USA.

Delrieu, M.-J. (1974) Simple explanation of the misses in the cooperation of charges in photosynthetic O₂ evolution. *Photochemistry and Photobiology* 20, 441–454.

Ducruet, J. M., and Vass, I. (2009). Thermoluminescence: experimental. *Photosynthesis Research* 101, 195–204.

Eaton-Rye, J. J. (2011). Construction of gene interruptions and gene deletions in the cyanobacterium *Synechocystis* sp. strain PCC 6803, in *Photosynthesis Research Protocols*, ed. R. Carpentier (Springer), 295–312.

Eaton-Rye, J. J., and Putnam-Evans, C. (2005). The CP47 and CP43 core antenna components, in *Photosystem II: The Light-Driven Water:Plastoquinone Oxidoreductase*, eds. T. J. Wydrzynski et al. (Springer), 45–70.

Eaton-Rye, J. J., Shand, J. A., and Nicoll, W. S. (2003). pH-dependent photoautotrophic growth of specific photosystem II mutants lacking luminal extrinsic polypeptides in *Synechocystis* PCC 6803. *FEBS Letters* 543, 148–153.

Eaton-Rye, J. J., and Vermaas, W. F. J. (1991). Oligonucleotide-directed mutagenesis of *psbB*, the gene encoding CP47, employing a deletion mutant strain of the cyanobacterium *Synechocystis* sp. PCC 6803. *Plant Molecular Biology* 17, 1165–1177.

Ferreira, K. N., Iverson, T. M., Maghlaoui, K., Barber, J., and Iwata, S. (2004). Architecture of the photosynthetic oxygen-evolving complex. *Science* 303, 1831–1838.

Jackson, S. A., and Eaton-Rye, J. J. (2015). Characterization of a *Synechocystis* sp. PCC 6803 double mutant lacking the CyanoP and Ycf48 proteins of Photosystem II. *Photosynthesis Research* 124, 217–229.

Jiang, H. B., Cheng, H. M., Gao, K. S., and Qiu, B. S. (2013). Inactivation of Ca²⁺/H⁺ exchanger in

This article is protected by copyright. All rights reserved.

Synechocystis sp. strain PCC 6803 promotes cyanobacterial calcification by upregulating CO₂-concentrating mechanisms. *Applied and Environmental Microbiology* 79, 4048–4055.

Joliot, P., and Joliot, A. (1968). A polarographic method for detection of oxygen production and reduction of Hill reagent by isolated chloroplasts. *Biochimica et Biophysica Acta - Bioenergetics* 153, 625–634.

Kaňa, R., Kotabová, E., Komárek, O., Šedivá, B., Papageorgiou, G. C., Govindjee, and Prášil, O. (2012). The slow S to M fluorescence rise in cyanobacteria is due to a state 2 to state 1 transition. *Biochimica et Biophysica Acta - Bioenergetics* 1817, 1237–1247.

Kirilovsky, D., Roncel, M., Boussac, A., Wilson, A., Zurita, J. L., Ducruet, J.-M., Bottin, H., Sugiura, M., Ortega, J. M., and Rutherford, A. W. (2004). Cytochrome *c*₅₅₀ in the cyanobacterium *Thermosynechococcus elongatus*: study of redox mutants. *Journal of Biological Chemistry* 279, 52869–52880.

Klughammer, C., and Schreiber, U. (1994). An improved method, using saturating light-pulses, for the determination of Photosystem-I quantum yield via P₇₀₀⁺-absorbance changes at 830 nm. *Planta* 192, 261–268.

Kok, B., Forbush, B., and McGloin, M. (1970). Cooperation of charges in photosynthetic O₂ evolution - I. A linear four step mechanism. *Photochemistry and Photobiology* 11, 457–475.

Morgan, T. R., Shand, J. a., Clarke, S. M., and Eaton-Rye, J. J. (1998). Specific requirements for cytochrome *c*₅₅₀ and the manganese-stabilizing protein in photoautotrophic strains of *Synechocystis* sp. PCC 6803 with mutations in the domain Gly-351 to Thr-436 of the chlorophyll-binding protein CP47. *Biochemistry* 37, 14437–14449.

Morris, J. N., Crawford, T. S., Jeffs, A., Stockwell, P. A., Eaton-Rye, J. J., and Summerfield, T. C. (2014). Whole genome re-sequencing of two “wild-type” strains of the model cyanobacterium *Synechocystis* sp. PCC 6803. *New Zealand Journal of Botany* 52, 36–47.

Morris, J. N., Eaton-Rye, J. J., and Summerfield, T. C. (2016). Environmental pH and the requirement for the extrinsic proteins of Photosystem II in the function of cyanobacterial photosynthesis. *Frontiers in Plant Science* 7, 1–8.

Morris, J. N., Eaton-Rye, J. J., and Summerfield, T. C. (2017). Phenotypic variation in wild-type substrains of the model cyanobacterium *Synechocystis* sp. PCC 6803. *New Zealand Journal of Botany* 55, 25–35.

This article is protected by copyright. All rights reserved.

- Nakamura, S., and Noguchi, T. (2015) Infrared detection of a proton released from tyrosine Y_D to the bulk upon its photo-oxidation in Photosystem II. *Biochemistry* 54, 5045–5053.
- Papageorgiou, G. C., and Govindjee (2011). Photosystem II fluorescence: slow changes - scaling from the past. *Journal of Photochemistry and Photobiology B: Biology* 104, 258–270.
- Putnam-Evans, C., Wu, J., and Bricker, T. M. (1996). Site-directed mutagenesis of the CP47 protein of photosystem II: alteration of conserved charged residues which lie within lethal deletions of the large extrinsic loop E. *Plant Molecular Biology* 32, 1191–1195.
- Rippka, R., Deruelles, J., Waterbury, J. B., Herdman, M., and Stanier, R. Y. (1979). Generic assignments, strain histories and properties of pure cultures of cyanobacteria. *Journal of General Microbiology* 111, 1–61.
- Robinson, H. H., and Crofts, A. R. (1983) Kinetics of the oxidation–reduction reactions of the Photosystem II quinone acceptor complex, and the pathway for deactivation. *FEBS Lett* 153, 221–226.
- Roose, J. L., Frankel, L. K., Mummadisetti, M. P., and Bricker, T. M. (2016). The extrinsic proteins of photosystem II: update. *Planta* 243, 889–908.
- Rutherford, A. W., Boussac, A., and Faller, P. (2004). The stable tyrosyl radical in Photosystem II: Why D? *Biochimica et Biophysica Acta - Bioenergetics* 1655, 222–230.
- Saito, K., Rutherford, A. W., and Ishikita, H. (2013). Mechanism of tyrosine D oxidation in Photosystem II. *Proceedings of the National Academy of Sciences* 110, 7690–7695.
- Sane, P. V (2004). Thermoluminescence, in *Photosynthesis Research Protocols*, ed. R. Carpentier (Totowa, NJ: Humana Press), 229–248.
- Shen, J.-R. (2015). The structure of photosystem II and the mechanism of water oxidation in photosynthesis. *Annual Review of Plant Biology* 66, 23–48.
- Shen, J.-R., Burnap, R. L., and Inoue, Y. (1995). An independent role of cytochrome c₅₅₀ in cyanobacterial photosystem II as revealed by double-deletion mutagenesis of the *psbO* and *psbV* genes in *Synechocystis* sp. PCC 6803. *Biochemistry* 34, 12661–12668.
- Sjöholm, J., Ho, F., Ahmadova, N., Brinkert, K., Hammarström, L., Mamedov, F., and Styring, S. (2017). The protonation state around Tyr_D/Tyr_D[•] in photosystem II is reflected in its biphasic oxidation kinetics. *Biochimica et Biophysica Acta - Bioenergetics* 1858, 147–155.

- Accepted Article
- Styring, S., Sjöholm, J., and Mamedov, F. (2012). Two tyrosines that changed the world: Interfacing the oxidizing power of photochemistry to water splitting in photosystem II. *Biochimica et Biophysica Acta - Bioenergetics* 1817, 76–87.
- Suga, M., Akita, F., Hirata, K., Ueno, G., Murakami, H., Nakajima, Y., Shimizu, T., Yamashita, K., Yamamoto, M., Ago, H., and Shen, J.-R. (2015). Native structure of photosystem II at 1.95 Å resolution viewed by femtosecond X-ray pulses. *Nature* 517, 99–103.
- Summerfield, T. C., Crawford, T. S., Young, R. D., Chua, J. P., Macdonald, R. L., Sherman, L. A., and Eaton-Rye, J. J. (2013). Environmental pH affects photoautotrophic growth of *Synechocystis* sp. PCC 6803 strains carrying mutations in the luminal proteins of PS II. *Plant and Cell Physiology* 54, 859–874.
- Summerfield, T. C., Eaton-Rye, J. J., and Sherman, L. A. (2007). Global gene expression of a Δ PsbO Δ PsbU mutant and a spontaneous revertant in the cyanobacterium *Synechocystis* sp. strain PCC 6803. *Photosynthesis Research* 94, 265–274.
- Summerfield, T. C., Shand, J. A., Bentley, F. K., and Eaton-Rye, J. J. (2005a). PsbQ (Sll1638) in *Synechocystis* sp. PCC 6803 is required for Photosystem II activity in specific mutants and in nutrient-limiting conditions. *Biochemistry* 44, 805–815.
- Summerfield, T. C., Winter, R. T., and Eaton-Rye, J. J. (2005b). Investigation of a requirement for the PsbP-like protein in *Synechocystis* sp. PCC 6803. *Photosynthesis Research* 84, 263–268.
- Umena, Y., Kawakami, K., Shen, J. R., and Kamiya, N. (2011). Crystal structure of oxygen-evolving photosystem II at a resolution of 1.9 Å. *Nature* 473, 55–60.
- Vass, I., Deák, Z., and Hideg, É. (1990). Charge equilibrium between the water-oxidizing complex and the electron donor tyrosine-D in Photosystem II. *Biochimica et Biophysica Acta - Bioenergetics* 1017, 63–69.
- Vass, I., and Govindjee (1996). Thermoluminescence from the photosynthetic apparatus. *Photosynthesis Research* 48, 117–126.
- Vass, I., Horvath, G., Herczeg, T., and Demeter, S. (1981). Photosynthetic energy conservation investigated by thermoluminescence. *Biochimica et Biophysica Acta - Bioenergetics* 634, 140–152.
- Vass, I., and Inoue, Y. (1986). pH dependent stabilization of $S_2Q_A^-$ and $S_2Q_B^-$ charge pairs studied by thermoluminescence. *Photosynthesis Research* 10, 431–436.

- Vass, I., Kirilovsky, D., and Etienne, A. L. (1999). UV-B radiation-induced donor- and acceptor-side modifications of photosystem II in the cyanobacterium *Synechocystis* sp. PCC 6803. *Biochemistry* 38, 12786–94.
- Vass, I., and Styring, S. (1991). pH-Dependent charge equilibria between tyrosine-_D and the S states in photosystem II. Estimation of relative midpoint redox potentials. *Biochemistry* 30, 830–839.
- Vinyard, D. J., Ananyev, G. M., Dismukes, C. G., and Charles Dismukes, G. (2013). Photosystem II: the reaction center of oxygenic photosynthesis. *Annual Review of Biochemistry* 82, 577–606.
- Wei, X., Su, X., Cao, P., Liu, X., Chang, W., Li, M., Zhang, X., and Liu, Z. (2016) Structure of spinach Photosystem II LHCII supercomplex at 3.2 Å resolution. *Nature* 536, 69–74.

Tables

Table 1. *Synechocystis* sp. PCC 6803 strains used in this work.

Strain	References	Antibiotics added to BG-11 plate culture
Wild type GT-O1	(Morris et al., 2014, 2017)	-
E364Q	(Morgan et al., 1998)	Kanamycin 25 µg/mL
ΔPsbV	(Morgan et al., 1998)	Erythromycin 25 µg/mL
E364Q:ΔPsbV	(Morgan et al., 1998)	Kanamycin 25 µg/mL + Erythromycin 25 µg/mL

Details about the creation of mutant strains and the GT-O1 wild type are available in the references indicated.

Table 2. Temperature of thermoluminescence peak maxima (T_{max}) and relative peak amplitude of *Synechocystis* sp. PCC 6803 strains.

Strain	Growth pH	- DCMU		+ DCMU	
		B band T_{max} ($^{\circ}$ C) (amplitude)	C band T_{max} ($^{\circ}$ C) (amplitude)	Q band T_{max} ($^{\circ}$ C) (amplitude)	C band T_{max} ($^{\circ}$ C) (amplitude)
Wild type	pH 7.5	30.25 \pm 2.2 (8060 \pm 1669)	51.7 \pm 2.4 (1549 \pm 737)	20.2 \pm 0.5 (10451 \pm 288)	52.65 \pm 0.2 (1750 \pm 263)
		pH 10.0	32.2 \pm 1.7 (7810 \pm 682)	54.15 \pm 0.9 (2397 \pm 1170)	20.0 \pm 1.7 (9212 \pm 461)
E364Q	pH 7.5		32 \pm 1.1 (11065 \pm 9266)	50.1 \pm 0.9 (5257 \pm 3553)	21.7 \pm 0.7 (29990 \pm 7604)
		pH 10.0	34.3 \pm 1.7 (15082 \pm 1755)	55.1 \pm 4.7 (6312 \pm 2520)	25.3 \pm 0.9 (19401 \pm 8550)
Δ PsbV	pH 7.5		29.8 ¹ (3070)	48.1 ¹ (550)	23.0 ¹ (6474)
		pH 10.0	29.7 ¹ (2481)	49.2 ¹ (901)	26.6 \pm 4.8 (3894 \pm 969)
E364Q: Δ PsbV	pH 7.5		28.7 \pm 0.2 (3831 \pm 1189)	49.65 \pm 1.6 (986 \pm 115)	26.91 \pm 0.8 (5599 \pm 2024)
		pH 10.0	37.1 \pm 6.8 (2133 \pm 840)	51.4 ¹ (1547)	29.5 \pm 1.0 (3774 \pm 1579)

Growth conditions: strains were assayed after 8 h in pH 7.5/pH 10.0 photoautotrophic conditions in the absence and presence of DCMU (mean \pm SEM, n = 3-5). ¹Fit based on a single curve due to signal to noise in these cells.

Table 3. Kinetics of single-turnover flash-induced chlorophyll fluorescence decay in *Synechocystis* sp. PCC 6803 strains.

Strain	Growth pH	+/- DCMU	Fast phase	Medium phase	Slow phase
			$t_{1/2}$ (μ s) [amp (%)]	$t_{1/2}$ (ms) [amp (%)]	$t_{1/2}$ (s) [amp (%)]
Wild type	7.5	-	174 \pm 17 (50 \pm 4.9)	1.5 \pm 0.4 (35 \pm 5.9)	1.3 \pm 0.11 (15 \pm 1.8)
	10.0	-	213 \pm 16 (59 \pm 1.4)	1.7 \pm 0.1 (30 \pm 2.5)	4.3 \pm 1.28 (11 \pm 2.1)
	7.5	+		2.5 \pm 0.9 (2.3 \pm 0.4)	0.6 \pm 0.04 (98 \pm 0.4)
	10.0	+		1.3 \pm 0.3 (3.1 \pm 1.1)	0.6 \pm 0.04 (97 \pm 1.1)
E364Q	7.5	-	253 \pm 18 (54 \pm 3.8)	2.1 \pm 0.2 (31 \pm 2.8)	9.5 \pm 3.99 (15 \pm 2.6)
	10.0	-	252 \pm 20 (49 \pm 3.7)	1.9 \pm 0.3 (32 \pm 2.5)	7.0 \pm 3.49 (18 \pm 1.8)
	7.5	+		4.1 \pm 2.3 (2.9 \pm 1.7)	1.1 \pm 0.08 (97 \pm 1.7)
	10.0	+		0.5 \pm 0.2 (2.1 \pm 0.4)	1.2 \pm 0.03 (98 \pm 0.4)
Δ PsbV	7.5	-	288 \pm 14 (68 \pm 3.4)	5.1 \pm 2.0 (19 \pm 5.2)	7.1 \pm 4.82 (12 \pm 3.0)
	10.0	-	259 \pm 56 (57 \pm 7.8)	4.5 \pm 1.6 (24 \pm 9.4)	6.1 \pm 2.47 (19 \pm 7.9)
	7.5	+		5.3 \pm 4.9 (5.2 \pm 2.2)	1.0 \pm 0.09 (95 \pm 2.2)
	10.0	+		5.1 \pm 3.3 (8.9 \pm 6.6)	1.0 \pm 0.01 (91 \pm 6.6)
E364Q: Δ PsbV	7.5	-	216 \pm 31 (40 \pm 8.7)	1.6 \pm 0.5 (36 \pm 6.6)	2.5 \pm 0.93 (24 \pm 7.8)
	10.0	-	165 \pm 21 (46 \pm 6.5)	1.3 \pm 0.2 (43 \pm 9.0)	1.5 \pm 0.27 (10 \pm 3.6)
	7.5	+		0.2 \pm 0.1 (8.8 \pm 2.5)	1.3 \pm 0.11 (91 \pm 2.1)
	10.0	+		0.7 \pm 0.3 (7.1 \pm 2.7)	1.5 \pm 0.19 (93 \pm 2.7)

Growth conditions: strains were grown to mid-late log-phase, incubated for 8 h in pH 7.5/photoautotrophic or pH 10.0/photoautotrophic conditions, and assayed in the absence and presence of DCMU (shaded rows). In the absence of DCMU, fast phase decay occurs due to Q_A^- to Q_B electron transfer in the presence of bound Q_B , medium phase decay represents Q_A^- to Q_B electron transfer where Q_B was not bound, and slow phase decay is due to charge recombination of $S_2Q_A^-/Q_B^-$. Fluorescence decay in the presence of DCMU, due to occupation of the Q_B site by DCMU, primarily occurs due to charge recombination of $S_2Q_A^-$. Times ($t_{1/2}$) and amplitudes (amp) were determined by curve fitting and are the average (\pm SEM) of 3-5 independent measurements.

Table 4. Analysis of the S-state distribution under different growth conditions and at pH 7.5 or pH 10.0.^a

Strain and treatment	S_0^b (%)	S_1 (%)	S_2 (%)	S_3 (%)	Misses [α] (%)	Double hits [β] (%)	$\sum S_{i,\text{dark}}^b$ (a.u.)	Y4/Y3
Mixotrophic growth at pH 7.5 ^d								
wild type	17.0	83.0	0	0	15.9	3.1	1.00	0.608
ΔPsbV	29.6	70.4	0	0	15.7	2.1	0.24	0.820
E364Q	10.0	90.0	0	0	15.0	2.8	0.59	0.490
E364Q: ΔPsbV	33.5	66.5	0	0	16.1	2.4	0.20	1.133
Photoautotrophic growth ^d								
wild type pH 7.5	16.1	83.9	0	0	14.3	2.0	0.96	0.564
wild type pH 10	14.0	86.0	0	0	14.7	2.6	0.70	0.583
E364Q pH 7.5	19.0	81.0	0	0	11.2	2.2	0.78	0.515
E364Q pH 10	24.2	78.8	0	0	14.1	7.2	0.55	0.660

^aOxygen evolution parameters were fit by using the matrix formalism of the Joliot-Kok model of O_2 evolution (Kok et al., 1970; Delrieu, 1974) in combination with a least square minimizing simplex algorithm.

^b $S_0 \dots S_3$ is the distribution of the S states in the dark and $\sum S_{i,\text{dark}}$ is the total number of active centers in any of the S states in the dark.

^cRatio of the O_2 yield on flash 4 to the O_2 yield on flash 3

^dStrains were grown in pH 7.5/mixotrophic conditions, and wild type and E364Q strains grown in photoautotrophic pH 7.5 and pH 10.0 conditions, for 24 h. The comparison of the fitted flash-induced oxygen evolution data to the experimental measurements is shown for the mixotrophically grown cells in supplemental Fig. S1 and for the photoautotrophically grown cells in supplemental Fig. S2.

Figure Captions

Fig. 1. Putative hydrogen bond network associated with Y_D of Photosystem II. The hydrophobic pocket surrounded by D2 Phe residues and Phe362 and Phe363 of CP47 is also depicted. The hypothesized hydrogen bond between CP47 Glu364 and D2 Arg294 is shown. The red spheres are the proximal and distal positions (with respect to the phenolic group of Y_D) of a single water located in the pocket. This water has been suggested to participate in proton coupled electron transfer when Y_D is oxidized by transferring the proton to D2 Arg180 (Saito et al., 2013; Nakamura and Noguchi, 2015). The figure was drawn using PyMOL (DeLano, 2002) and PDB4UB6 (Suga et al., 2015).

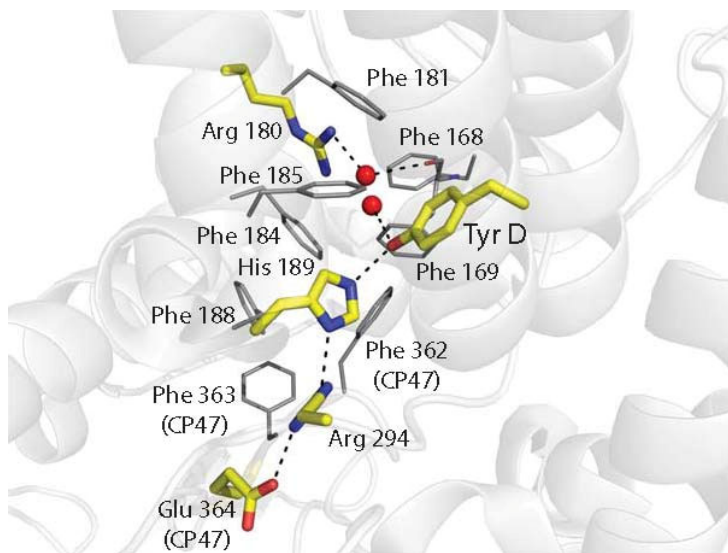
Fig. 2. Photosynthetic thermoluminescence from *Synechocystis* sp. PCC 6803 strains incubated for 8 h in pH 7.5 (dashed lines) or pH 10.0 (solid lines) under photoautotrophic conditions. Measurements were made in the absence (panels A and B) and presence (panels C and D) of DCMU. Traces represent the mean photon count from 3-5 independent measurements. (A, C) Wild type = black, E364Q = red. (B, D) Δ PsbV = blue, and E364Q: Δ PsbV = green.

Fig. 3. Fluorescence decay following a single-turnover actinic flash in *Synechocystis* sp. PCC 6803 strains incubated for 8 h in pH 7.5 (dashed lines) or pH 10.0 (solid lines) under photoautotrophic conditions. Measurements were made in the absence (panels A and B) and presence (panels C and D) of DCMU. Traces represent the mean of 3-5 independent measurements. (A, C) Wild type = black, E364Q = red. (B, D) Δ PsbV = blue, and E364Q: Δ PsbV = green.

Fig. 4. Flash-induced oxygen evolution (panels A and B), fluorescence induction (panel C), and P_{700} oxidation state (panel D) of *Synechocystis* sp. PCC 6803 strains. Cells were incubated for 24 h (panel A) and 8 h (panels C and D) in pH 7.5 (dashed lines) or pH 10.0 (solid lines) under mixotrophic conditions, or incubated for 24 h in pH 7.5 in photoautotrophic conditions (panel B). (A, B) Flash-induced oxygen evolution during exposure of dark-adapted cells to 20 saturating, single-turnover actinic flashes at 617 nm/4 Hz. A representative trace following 3-4 independent measurements is shown; data were normalized to the first flash value. Flash-induced oxygen evolution was not measured for Δ PsbV and E364Q: Δ PsbV cells under photoautotrophic conditions. In panel A the data for the first 13 flashes are plotted for the Δ PsbV mutant due to the noise arising as a result of the

This article is protected by copyright. All rights reserved.

reduced number of PS II centers in these cells. (C) Fluorescence induction following the exposure of dark-adapted cells to actinic 639 nm light; traces represent the mean of 3-4 independent measurements. (D) P_{700} oxidation was induced after 0.5 s by exposure of dark-adapted cells to actinic 635 nm light; values reflect absorbance change in the near-infrared ($A_{875\text{ nm}} - A_{830\text{ nm}}$), and were normalized to the signal maxima ($\sim 100\% P_{700}^+$) and represent the mean of 3-4 independent measurements. In all panels the strains are: wild type (black), E364Q (red), Δ PsbV (blue), and E364Q: Δ PsbV (green). In panel A and B the symbols are: wild type, black circles; E364Q, red squares; Δ PsbV, blue diamonds, and E364Q: Δ PsbV, green triangles. In panel B empty symbols are pH 7.5 and filled symbols are pH 10.



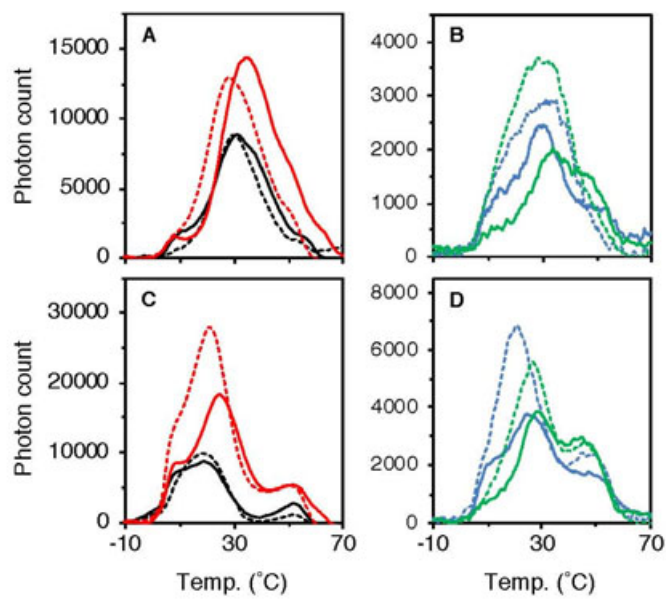


Figure 2

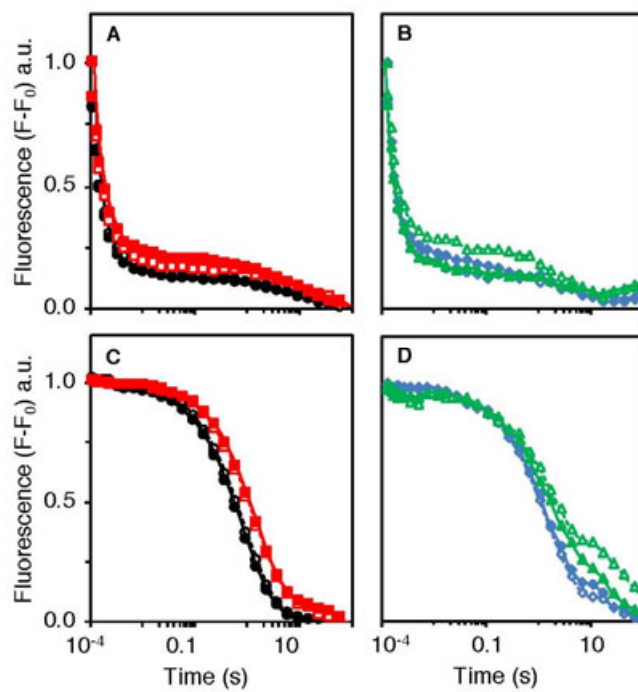


Figure 3

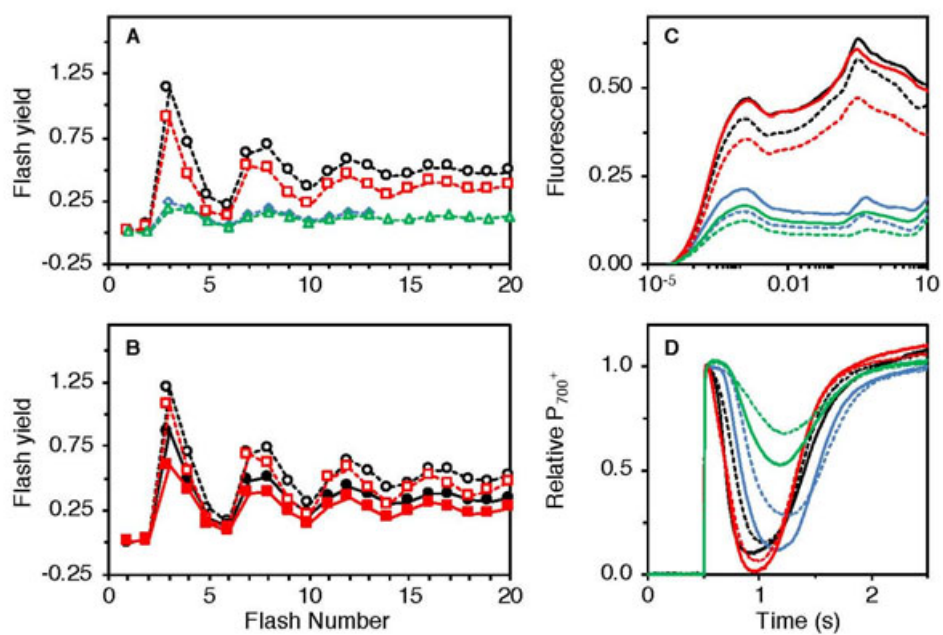


Figure 4